

Acoustic emission source modeling

P. Hora^{a,*}, O. Červená^a

^a*Institute of Thermomechanics of the ASCR, v.v.i., Veleslavínova 11, 301 14 Plzeň, Czech Republic*

Received 27 August 2009; received in revised form 13 May 2010

Abstract

The paper deals with the acoustic emission (AE) source modeling by means of FEM system COMSOL Multiphysics. The following types of sources are used: the spatially concentrated force and the double forces (dipole). The pulse excitation is studied in both cases. As a material is used steel. The computed displacements are compared with the exact analytical solution of point sources under consideration.

© 2010 University of West Bohemia. All rights reserved.

Keywords: acoustic emission source, wave propagation, FEM

1. Introduction

Growth of cracks is important AE source, and the study of the waves they generate has played a major role in our understanding of the inner structure of the materials and the nature of the AE source. Energy release during growth of crack can be simulated by the concentrated force or concentrated force moment [1, 3, 9, 10]. This work focuses on modeling a concentrated source located in an infinite domain. The steel cylinder (radius 50 mm, height 100 mm) is used for the infinite domain simulation, see fig. 1. To provide a point of comparison for the finite element models, an analytical solutions for displacements in unbounded media excited a concentrated sources are also mentioned.

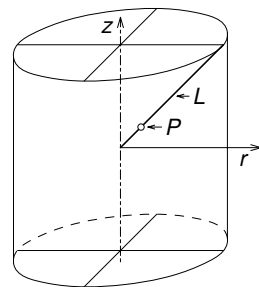


Fig. 1. Geometry

2. Point sources in unbounded homogeneous media

The simplest problem corresponds to a spatially concentrated force (or point source) directed along one of the coordinate axes. Even in this case, however, solving the elastic wave equation is a rather complicated task that requires considerable mathematical background. The starting point is the scalar wave equation with a source term, which is first solved for an impulsive source, in which case the solution is known as Green's function for the problem. Then the Helmholtz decomposition theorem is used to reduce the solution of the elastic wave equation to the solution of two simpler ones. After this series of steps, and considerable additional work, the problem of the concentrated force can be solved. Then it is relatively easy to investigate the problem involving pairs of parallel forces of equal magnitude and opposite directions a small distance apart. This combination of forces is extremely important because it allows the introduction of the concept of a moment tensor, which plays a fundamental role in the theory.

*Corresponding author. Tel.: +420 377 236 415, e-mail: hora@cdm.it.cas.cz.

We consider elastic wave equation $\rho \ddot{\mathbf{u}} = (\lambda + 2\mu)\nabla(\nabla \cdot \mathbf{u}) - \mu\nabla \times (\nabla \times \mathbf{u}) + \mathbf{f}$, where \mathbf{u} is displacement, ρ is the material density, λ, μ are Lamé elastic constants and \mathbf{f} represents the source force.

2.1. Concentrated force

Initially, we focused on the simplest case – concentrated force in direction of along one of the coordinate axes.

Using the notation u_{ij} to represent the displacement in the i -direction due to a concentrated point force $\mathbf{f}(\mathbf{x}, t; \boldsymbol{\xi})$ applied in the j -direction at the point $\boldsymbol{\xi}$ ($\mathbf{f}(\mathbf{x}, t; \boldsymbol{\xi}) = f_0(t)\delta(\mathbf{x} - \boldsymbol{\xi})\mathbf{e}_j$, see fig. 2 for case $j = 3$), the displacements over the domain may be determined by evaluating the following equation [1, 4, 10]:

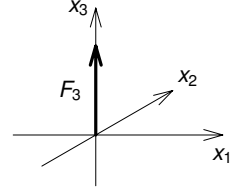


Fig. 2. The point force

$$4\pi\rho u_{ij}(\mathbf{x}, t) = \frac{3\gamma_i\gamma_j - \delta_{ij}}{R^3} \int_{R/\alpha}^{R/\beta} \tau f_0(t - \tau) d\tau + \frac{\gamma_i\gamma_j}{\alpha^2 R} f_0\left(t - \frac{R}{\alpha}\right) - \frac{\gamma_i\gamma_j - \delta_{ij}}{\beta^2 R} f_0\left(t - \frac{R}{\beta}\right) \quad (1)$$

where ρ is the material density, $R = |\mathbf{x} - \boldsymbol{\xi}|$ is the distance from the source, $\gamma_i = (x_i - \xi_i)/R$ are the direction cosines of vector, δ_{ij} is the Kronecker delta, $\alpha^2 = c_P^2 = (\lambda + 2\mu)/\rho$ and $\beta^2 = c_S^2 = \mu/\rho$ represent squares of the speeds of pressure and shear waves, respectively. In these equations, λ, μ are Lamé elastic constants and $f_0(t)$ represents the source force.

2.2. Concentrated couples and dipoles

Pairs of parallel forces of equal magnitude and opposite directions some distance apart are considered. The forces parallel to the coordinate axes separated by very small distances are represented as double forces. If the two forces have different lines of action they constitute a couple; otherwise they constitute a dipole. Let $M_{ij}(t)$ be the moment of either the dipole in the x_i direction ($i = j$) or the couple with forces and arm in the x_i and x_j directions, respectively ($i \neq j$). For dipole case $i = j = 3$ see fig. 3. $M_{ij}(t) = f_0(t)\bar{M}_{ij}$, where $f_0(t)$ is same as in previous section and \bar{M}_{ij} is a component of tensor that describes the spatial nature of the source. Using the notation $u_{ijk}(\mathbf{x}, t)$ to represent the displacement in the k -direction due to moment $M_{ij}(t)$ applied at the point $\boldsymbol{\xi}$, the displacements over the domain may be determined by evaluating the following equation [1, 4, 10]:

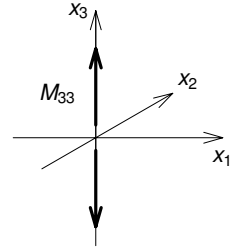


Fig. 3. The dipole

$$\begin{aligned} 4\pi\rho u_{ijk}(\mathbf{x}, t) = & (15\gamma_k\gamma_i\gamma_j - 3\gamma_k\delta_{ij} - 3\gamma_i\delta_{kj} - 3\gamma_j\delta_{ki}) \frac{1}{R^4} \int_{R/\alpha}^{R/\beta} \tau M_{ij}(t - \tau) d\tau \\ & + (6\gamma_k\gamma_i\gamma_j - \gamma_k\delta_{ij} - \gamma_i\delta_{kj} - \gamma_j\delta_{ki}) \frac{1}{\alpha^2 R^2} M_{ij}\left(t - \frac{R}{\alpha}\right) \\ & - (6\gamma_k\gamma_i\gamma_j - \gamma_k\delta_{ij} - \gamma_i\delta_{kj} - 2\gamma_j\delta_{ki}) \frac{1}{\beta^2 R^2} M_{ij}\left(t - \frac{R}{\beta}\right) \\ & + \gamma_k\gamma_i\gamma_j \frac{1}{\alpha^3 R} \dot{M}_{ij}\left(t - \frac{R}{\alpha}\right) - (\gamma_k\gamma_i - \delta_{ki}) \gamma_j \frac{1}{\beta^3 R} \dot{M}_{ij}\left(t - \frac{R}{\beta}\right) \end{aligned} \quad (2)$$

where $\rho, R, \gamma_i, \delta_{ij}, \alpha$ and β have the same meaning as in previous section.

The used source force is:

$$f_0(t) = at \exp(-bt), \quad (3)$$

where a and b are parameters controlling duration and amplitude of the source. Examples for various parameters a and b which are used in following simulations are shown in fig. 4 – top, the normalized power spectra of used source forces are shown in fig. 4 – bottom, $S(f)$ is power spectrum.

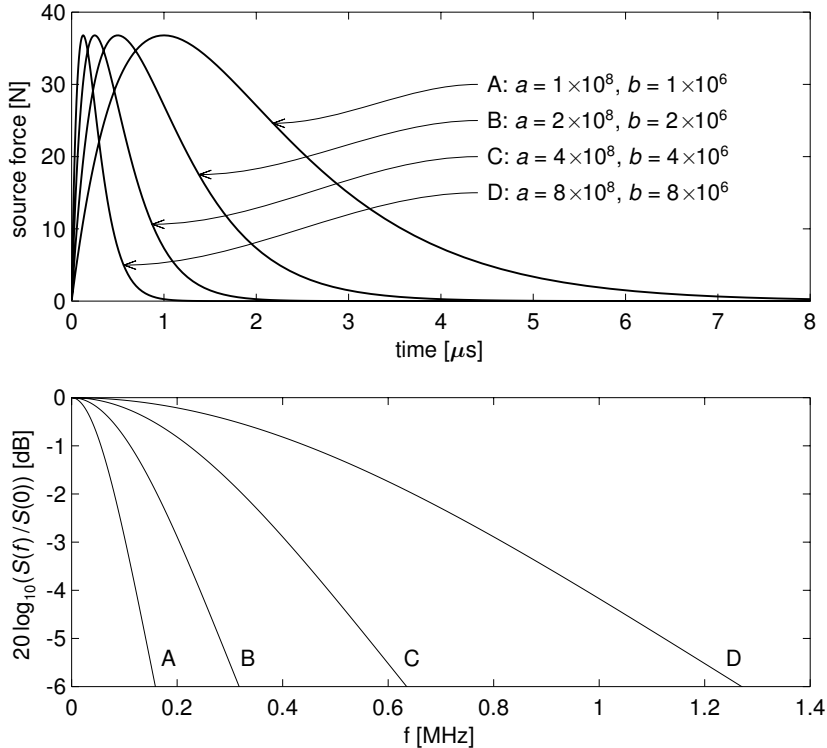


Fig. 4. The source force $f_0(t) = at e^{-bt}$ (top) and its normalized power spectrum (bottom)

3. Comparison FEM versus analytical solution

FEM calculations are performed in the commercial environment COMSOL Multiphysics with the Structural Mechanics Module [5]. The finite element discretization of the time-dependent PDE problem leads to an ODE system. COMSOL Multiphysics uses solver DASPCK created by Linda Petzold at the University of California, Santa Barbara. The DASPCK solver is based on the older code DASSL, which uses variable-order variable-stepsize backward differentiation formulas (BDF). Thus the solver is an implicit time-stepping scheme, which implies that it must solve a possibly nonlinear system of equations at each time step. It solves the nonlinear system using a Newton iteration, and it then solves the resulting system with an arbitrary COMSOL Multiphysics linear solver. The order of BDF is chosen 5 and as the linear system solver is used UMFPAK.

Because of the axial symmetry of the geometry, an axisymmetric 2D application mode is used. Elements are the Lagrange-Quadratic type. The time dependent analysis is realized. The time stepping parameters are: times (from 0 to 8 μs with step 0.01 μs), relative tolerance (10^{-5}) and absolute tolerance (10^{-10}). No damping is used. The prescribed exciting force is given by a function (see fig. 4 – top).

A mapped quad mesh is created. For acoustic emission applications the max. frequency is about 1 MHz. The 6dB bandwidth for the time function of source force A, B, and C is under this limit, see fig. 4 – bottom. The shortest relevant wavelength is: $\lambda = c/f \approx 6$ mm, where $c = 5950$ m/s is the speed of longitudinal wave in steel and $f = 1$ MHz is the max. frequency. FE rules for transients state that: six quadratic elements per wavelength should yield an accuracy less than a few percent [2, 6]. Therefore the size of one mesh element is chosen 0.5×0.5 mm, see fig. 5.

For model of concentrated force, number of elements is 20 000 and number of degree of freedom is 161 202. For model of dipole force, the half of model is enough due to the symmetry. Therefore number of elements is 10 000 and number of degree of freedom is 80 802.

The studied material is steel with Young’s modulus $E = 200$ GPa, Poisson’s ratio $\nu = 0.29$ and density $\rho = 7870$ kg/m³. For postprocessing, the line L is given by relations $z = r$ and the point P has coordinates [$z = 1$ cm, $r = 1$ cm], see fig. 1.

3.1. Concentrated force

The point, circle area (radius $q = 0.5$ mm) and cylinder (radius $q = 0.5$ mm, height $h = 1$ mm) are used to FEM-modeling of point force in the z direction (see fig. 5). In case of point, the excitation is applied in origin (fig. 5 a) as *point* load by source force $f_0(t)$ in direction z , see eq. (3). In case of circle area, the excitation is applied on edge (bold line in fig. 5 b) as *edge* load by force in direction z . Thus the source force must be divided by the circle area:

$$\bar{f}_0(t) = f_0(t)/(\pi q^2). \tag{4}$$

In case of cylinder, the excitation is applied on subdomain (black rectangle in fig. 5 c) as *body* load by force in direction z . The source force must be divided by the volume of cylinder:

$$\tilde{f}_0(t) = f_0(t)/(\pi q^2 h). \tag{5}$$

The constraint boundary condition is axial symmetry on the symmetry axis z marked by number 1 in fig. 5 d, and other boundary conditions of model on boundaries 2–4 are free due to modeling infinite domain in axisymmetric 2D application mode. The neighbourhood of source is remarked by circle and letter s .

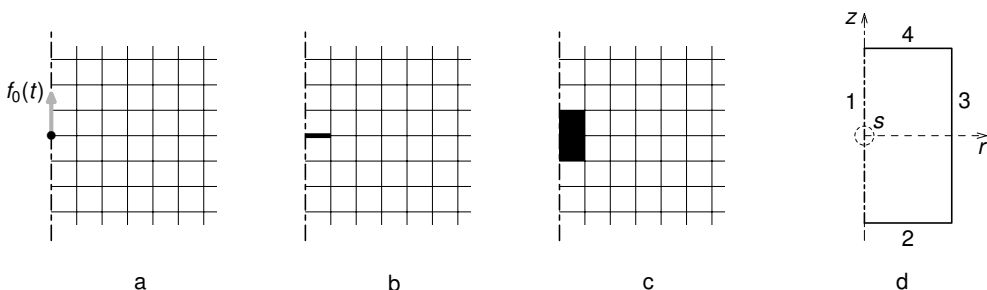


Fig. 5. FEM-models of force: a – point, b – circle area and c – cylinder; d – the boundary of model

The solution times and accuracies of the tasks are too different. The root mean square errors of displacements are computed to comparison of the model usability. The root mean square error is defined as

$$\text{RMSE } w = \sqrt{\frac{\sum_{n=1}^N (w_n^{FEM} - w_n^T)^2}{N}}, \quad (6)$$

where w_n^{FEM} is n^{th} observation of variable w obtained by FE-axisymmetric model, w_n^T is n^{th} observation of theoretical variable w and N is number of observations.

The values of the root mean square error for radial displacement (RMSE u_r) and vertical displacement (RMSE u_z) in time $6 \mu\text{s}$ over the line L for the three source models and for four types of time function (see fig. 4 – top) are included in tab. 1. In this table the solution times of particular tasks are shown too. Although the solution times for cylinder model are the shortest, the circle area model will be used for concentrated force modeling in future simulations because of its the smallest RMSE.

Fig. 6 shows space distribution of absolute errors for time function type A. The analytical solution (1) of radial ($u_r = u_{13}$) and vertical ($u_z = u_{33}$) displacements at time $6 \mu\text{s}$ over the line L is shown in upper-left picture. The other pictures of this figure show absolute errors of FE-solution for particular sources: point, circle area and cylinder. The source model is represented by symbol in bottom-left corner of particular pictures.

The effect of the exciting pulse width for circle area source model is demonstrated for time $6 \mu\text{s}$ over the line L in fig. 7 and for time dependence in point P in fig. 8. The solid lines are used for radial displacements and the dashed lines for vertical displacements in both of figures. Color of lines determines kind of solution. Gray is used for analytical and black for FEM solutions. The type of time function is represented by letter in upper-left corner of particular

Table 1. Comparison of solution times and RMSE for the particular time function types and source models

Model of source	Parameters	Type of function			
		A	B	C	D
•	RMSE u_r [10^{-10} m]	0.045 9	0.092 7	0.184 1	0.925 0
	RMSE u_z [10^{-10} m]	0.048 6	0.094 1	0.190 9	0.944 2
	Solution time [s]	2 936	3 667	4 787	9 668
	RMSE u_r [10^{-10} m]	0.032 8	0.079 0	0.148 9	0.264 0
	RMSE u_z [10^{-10} m]	0.033 9	0.082 4	0.150 1	0.266 1
	Solution time [s]	865	1 586	1 793	2 227
	RMSE u_r [10^{-10} m]	0.063 7	0.089 8	0.763 6	0.798 0
	RMSE u_z [10^{-10} m]	0.066 6	0.091 2	0.778 4	0.803 9
	Solution time [s]	713	789	1 356	1 765

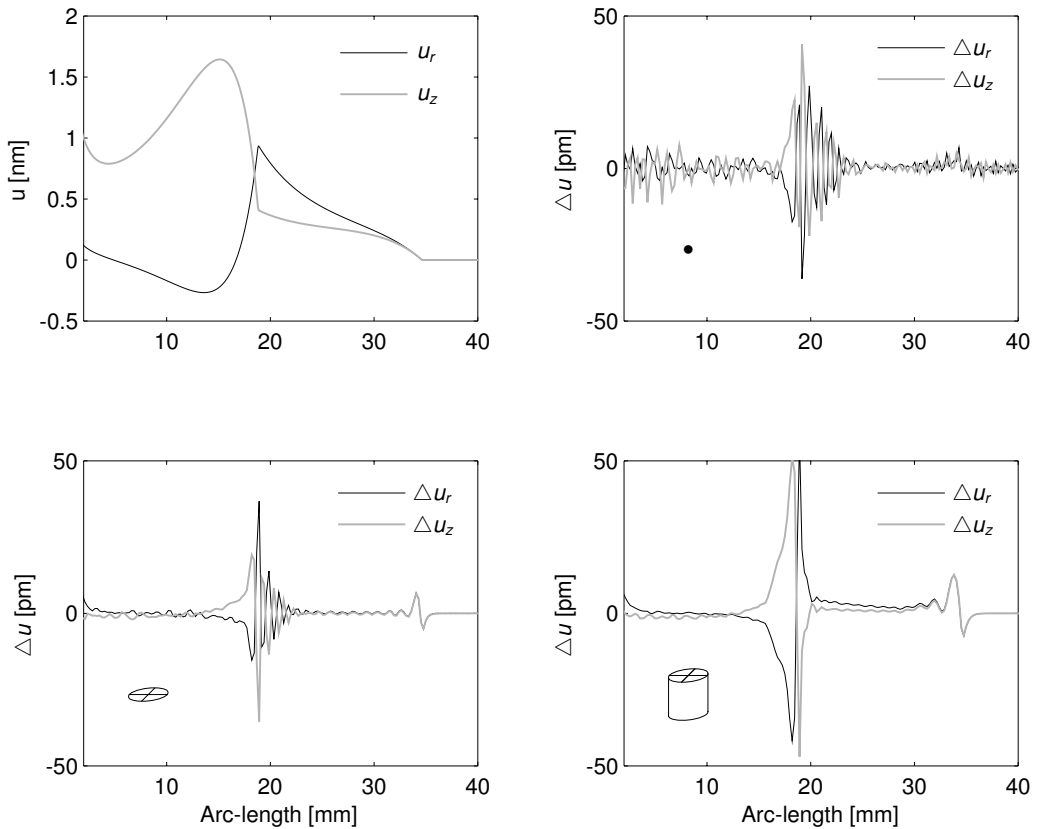


Fig. 6. Comparison of radial (u_r) and vertical (u_z) displacements for FE-axisymmetric models to an analytical solution for the time function type A at time $6 \mu s$ over the line L . Upper left: analytical solution; the others: absolute errors of FE-solution for particular sources: point, circle area and cylinder

pictures. These results shows the ability of COMSOL Multiphysics to represent *accurately* the wave except for minor variations at the peak of the wave and at neighbourhood of suddenly changes, which are appeared in cases of the time function type C and D with the narrower pulse width. These differences are due to the dispersive properties of used mesh and the frequency content of used excitation [7].

3.2. Concentrated dipole

Analogous to the previous case the point, circle area (radius $q = 0.5 \text{ mm}$) and cylinder (radius $q = 0.5 \text{ mm}$, height $h = 1 \text{ mm}$) are used to FEM-modeling of dipole. With respect to symmetry of the loading forces it is possible to analyze only upper half of model (see fig. 9). Four cases of the dipole arm length (from 1 to 4 mm) are computed in FEM simulations. The influence of the dipole arm length d is studied. In case of point, the excitation is applied in point with coordinates $[0, d/2]$ as *point* load by source force $f_0(t)$ in direction z , see eq. (3). In case of circle area, the excitation is applied on edge (bold line in fig. 9 b) as *edge* load $\bar{f}_0(t)$ in direction z , see eq. (4).

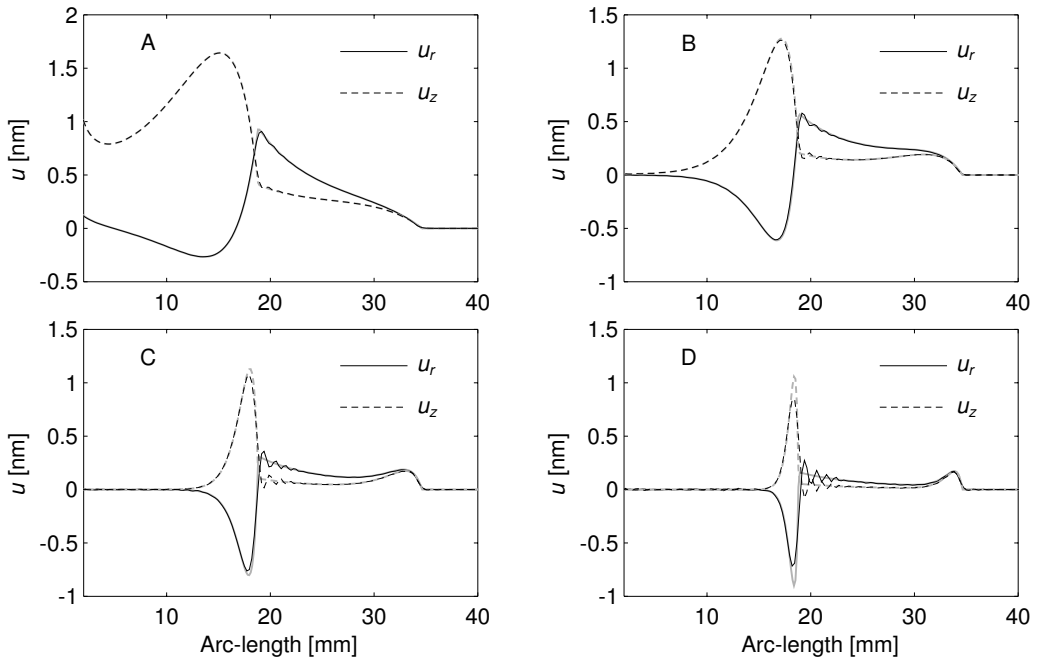


Fig. 7. Comparison of displacements for a FE model to an analytical solution for the circle source with the time function A, B, C, and D at time $6 \mu\text{s}$ over the line L . Analytical: gray; FEM: black

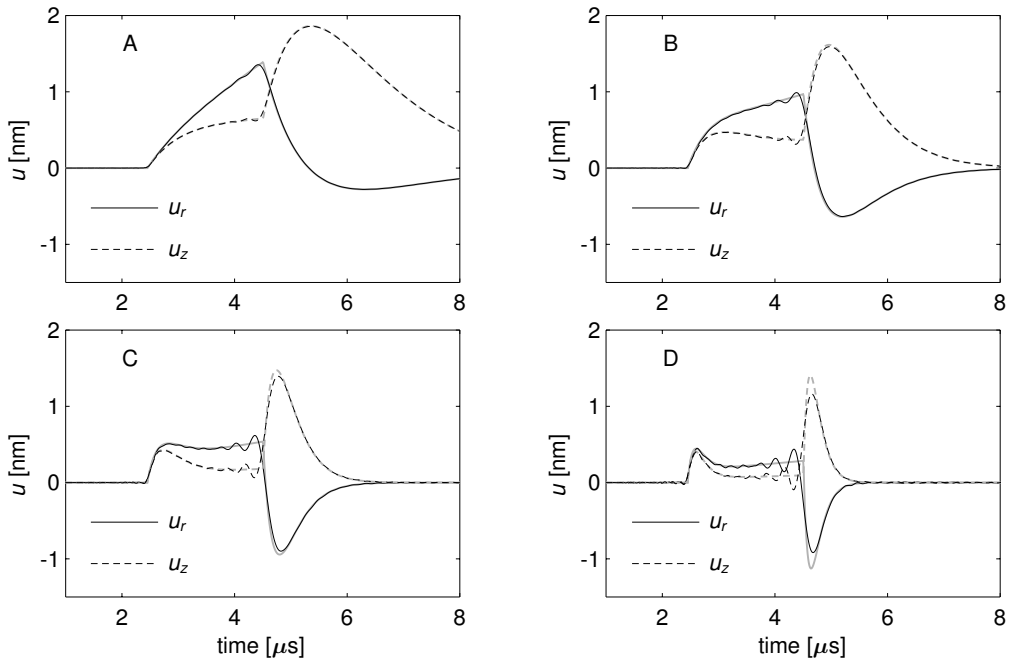


Fig. 8. Comparison of displacements for a FE model to an analytical solution for the circle source with the time function A, B, C, and D in point P . Analytical: gray; FEM: black

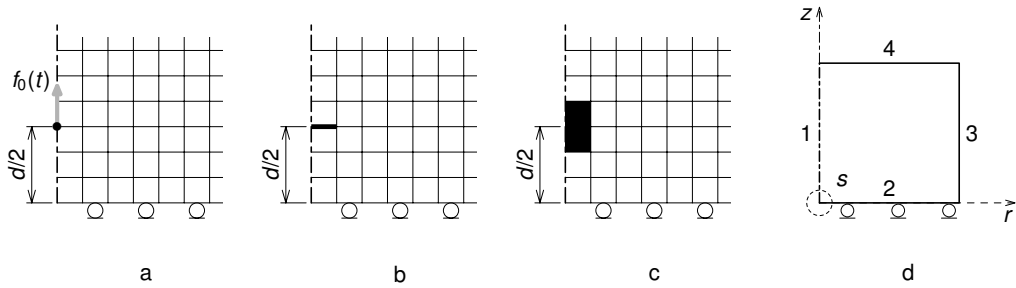


Fig. 9. FEM-models of dipole: a – point, b – circle, c – cylinder (here d is the arm length); d – the boundary of model

In case of cylinder, the excitation is applied on subdomain (black rectangle in fig. 9 c) as *body load* $\tilde{f}_0(t)$ in direction z , see eq. (5).

The constraint boundary conditions: i) axial symmetry on the axis z (dot-dash line) marked by number 1 in fig. 9 d; ii) the symmetry plane on the axis r (roller symbols) marked by number 2; iii) free boundary condition marked by numbers 3–4 due to modeling infinite domain in axisymmetric 2D application mode. The neighbourhood of source is remarked by circle and letter s .

Table 2. Comparison solution time and root mean square error (RMSE) for the particular time function type and for particular source models

Model of source	Parameters	Type of function			
		A	B	C	D
•	RMSE u_r [10^{-6} m]	0.024 8	0.048 0	0.119 7	0.170 2
	RMSE u_z [10^{-6} m]	0.024 8	0.048 0	0.119 3	0.170 5
	Solution time [s]	1 769	1 696	2 603	2 583
⊖	RMSE u_r [10^{-6} m]	0.032 3	0.076 9	0.084 3	0.168 8
	RMSE u_z [10^{-6} m]	0.032 2	0.076 8	0.083 8	0.169 0
	Solution time [s]	911	928	631	923
⊖	RMSE u_r [10^{-6} m]	0.024 2	0.075 6	0.118 9	0.162 4
	RMSE u_z [10^{-6} m]	0.024 1	0.075 3	0.118 3	0.161 8
	Solution time [s]	470	417	413	420

Again, the values of RMSE u_r and RMSE u_z , see eq. (6), in time $6 \mu\text{s}$ over the line L for the source models and for four types of time function are included in tab. 2. The solution times of particular tasks are shown there too. The values in this table are only for the 1 mm arm length dipole. The solution times for cylinder model are the shortest as well as in case of point concentrated force. The RMSE values are not so unique as in case point concentrated force, but their differences are not so big in comparison with differences in solution times. Therefore the cylinder model will be used for concentrated dipole modeling in future simulations.

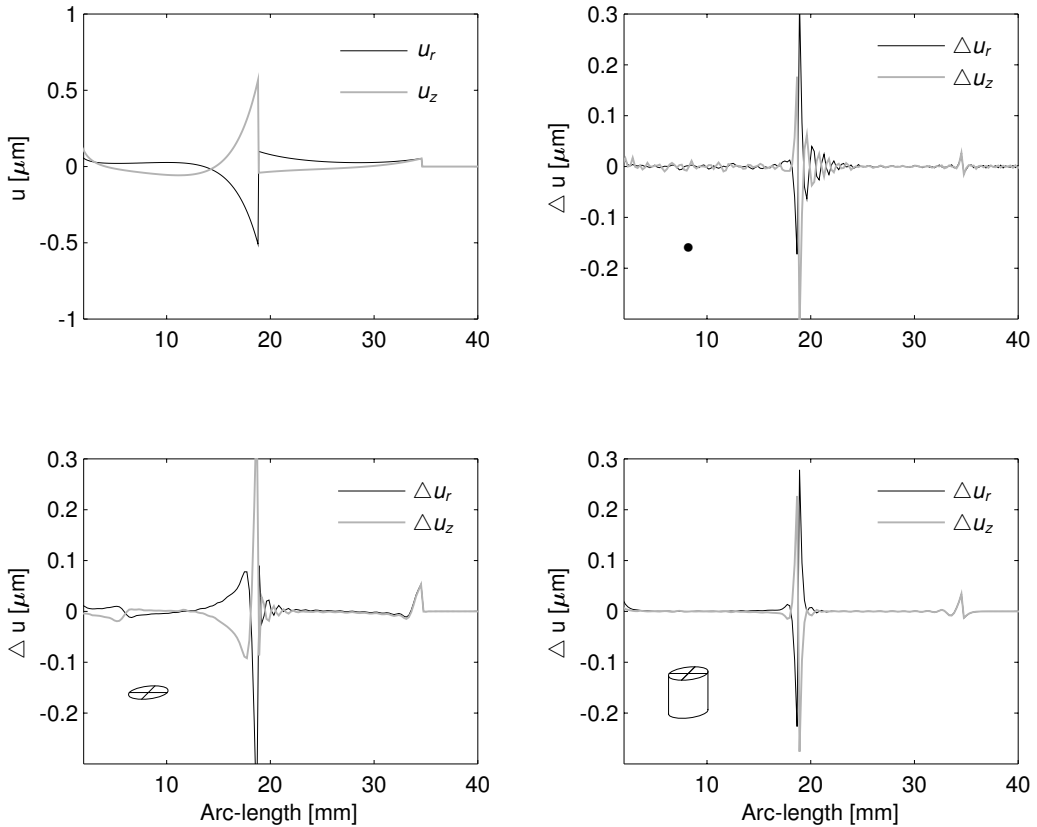


Fig. 10. Comparison of radial (u_r) and vertical (u_z) displacements for FE-axisymmetric models to an analytical solution for the time function type A at time $6 \mu\text{s}$ over the line L . Upper left: analytical solution; the others: absolute errors of FE-solution for particular sources: point, circle area and cylinder

Fig. 10 shows space distribution of absolute errors for time function type A and dipole arm length 1 mm. The analytical solution (2) of radial ($u_r = u_{331}$) and vertical ($u_z = u_{333}$) displacements at time $6 \mu\text{s}$ over the line L is shown in upper-left picture of fig. 10. The other pictures of this figure show absolute errors of FE-solution for particular sources: point, circle area and cylinder. The source model is represented by symbol in bottom-left corner of particular pictures.

The effect of the dipole arm length for cylinder source model and time function A is demonstrated for time $6 \mu\text{s}$ over the line L in fig. 11 and for time dependence in point P in fig. 12. The solid lines are used for radial displacements and the dashed lines for vertical displacements in both of figures. Color of lines determines kind of solution. Gray is used for analytical and black for FEM solutions. The difference between FEM and analytical solution (2) is decreasing with the decreasing arm length. The analytical solution supposes that the arm of dipole is infinitesimal. In order to be able to compare the analytical and FEM solution, the FEM solution is divided by the dipole arm length. Roughly speaking, FEM solution very well represents the wave arrival, especially for the smallest arm length.

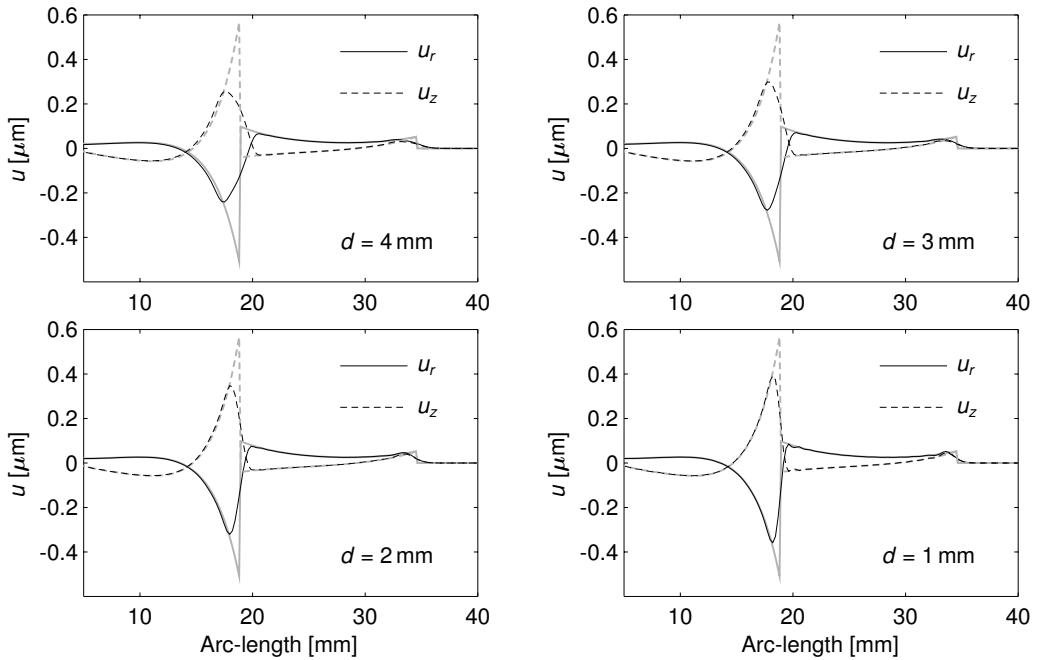


Fig. 11. Comparison of displacements for a FE model to an analytical solution for the cylindrical dipole source with the time function A at time $6 \mu\text{s}$ over the line L for particular arm lengths d . Analytical: gray; FEM: black

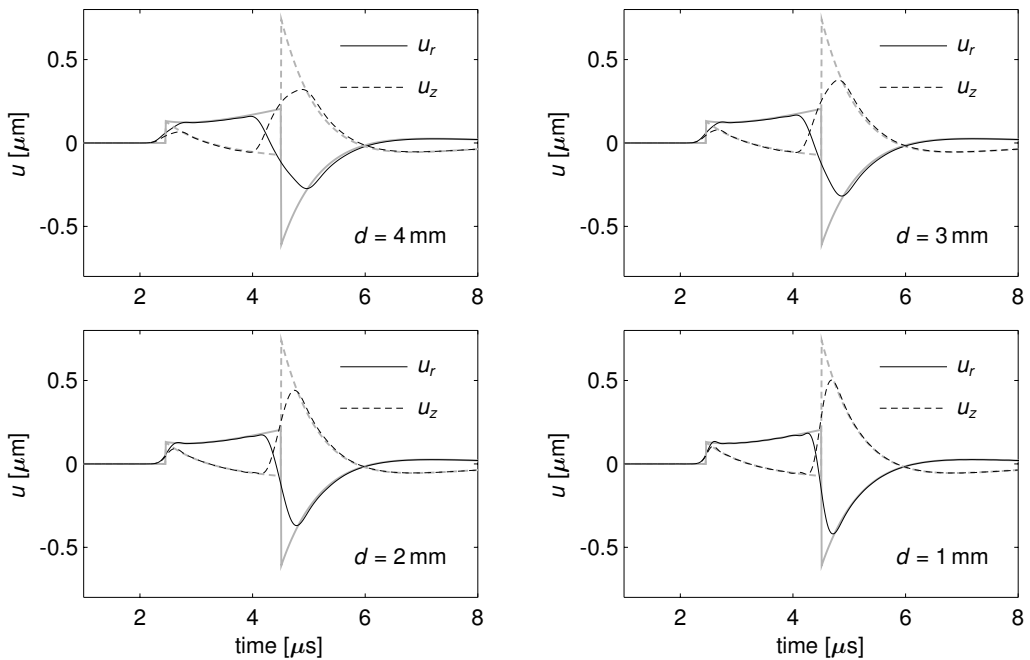


Fig. 12. Comparison of displacements for a FE model (black) to an analytical solution (gray) for the cylindrical dipole source with the time function A in point P for some arm lengths d

4. Conclusion

The acoustic emission source modeling by means of FEM system COMSOL Multiphysics [5] is presented here. The spatially concentrated force and concentrated dipole are used as kinds of the acoustic emission sources. Four kinds of the time dependence loading are studied. As a model of unbounded media is used the steel cylinder.

To provide a point of comparison for the finite element models, an analytical solutions for displacements in unbounded media excited a concentrated sources are also computed. MATLAB [8] is used for these computations, scripting of COMSOL tasks and figure creating.

Several various shapes (point, circle area and cylinder) are used to FEM-modeling of point force. In comparison with the analytical solution, the circle area exciting gives the smallest root square mean errors. Therefore the circle area model will be used for concentrated force modeling in our future simulations. The effect of the exciting pulse width is analyzed. The computed displacements show the ability of COMSOL Multiphysics to represent accurately the wave propagation. There are a minor variations at the peak of the waves and at neighbourhood of suddenly changes. These differences are due to dispersive properties of mesh.

To FEM-modeling of dipole forces are used the same shapes. In comparison with the analytical solution, the cylinder exciting has the smallest solution time with acceptable root square mean errors. Therefore the cylinder model will be used for concentrated dipole modeling in our future simulations. The influence of the dipole arm length d is studied. Four cases of the dipole arm length (1, 2, 3, and 4 mm) are computed in FEM simulations. The difference between FEM and analytical solution (the arm length of dipole is infinitesimal) is decreasing with the decreasing arm length. FEM solution very well represents the wave arrival, especially for the smallest arm length.

The proper motivation of this study is choosing the best model of concentrated force and dipole. These models will be used to calculations of surface displacements in real steel constructions for the purpose of comparing with surface displacements obtained by non destructive testing.

All computations are performed on HP xw6600 Workstation with two processors Intel Xeon E5430/2.67 GHz (Quad Core) and 32 GB RAM.

Acknowledgements

The work has been supported by the Institute Research Plan AV0Z20760514 and by the grants GA CR No 101/09/1630.

References

- [1] Aki, K., Richards, P. G., Quantitative seismology, 2nd ed., University Science Books, Sausalito, California, 2002.
- [2] Burnett, D. S., Finite Element Analysis, Addison-Wesley, 1988.
- [3] Ceranoglu, A., Pao, Y.-H., Propagation of elastic pulses and acoustic emission in a plate: Part I, II, III, J. Appl. Mech., 1981, Vol. 48, pp. 125–147.
- [4] Chapman, Ch., Fundamentals of seismic wave propagation, Cambridge University Press, 2006.
- [5] COMSOL, Inc., <http://www.comsol.com>
- [6] Ihlenburg, F., Finite Element Analysis of Acoustic Scattering, Springer, 1998.
- [7] Kolman, R., Dispersion properties of plane square serendipity finite element in elastodynamics, PhD. thesis, ČVUT Praha, 2009, (in Czech).

- [8] The MathWorks, Inc., <http://www.mathworks.com>
- [9] Pao, Y.-H., Gajewski, R. R., The generalized ray theory and transient responses of layered elastic solids, *Physical Acoustics. Principle and Methods.*, Vol. 13, Chap. 6, Academic Press New York, 1977, ed. R. N. Thurston.
- [10] Pujol, J., *Elastic wave propagation and generation in seismology*, Cambridge University Press, 2003.